Sensors & Transducers, Vol. 168, Issue 4, April 2014, pp. 249-259

Sensors & Transducers

A New Approach to Establishing Cathode Rod Temperature-current Model Based on Nickel Electrolysis Cells

[1, 2] Ren-Tao Zhao, [2] Li-Ming Lin, [1] Hua-De Li, [2] You-Yu Wang, [2] Jun Tie
[1] School of Automation and Electrical Engineering, University of Science & Technology Beijing
[2] North China University of Technology, Beijing, 100144, China
[1] Tel.: 18611784376

Received: 19 January 2014 /Accepted: 7 March 2014 /Published: 30 April 2014

Abstract: When different current flows through the cathode rod, the rod temperature distribution shows different trends in nickel electrolysis cells. The rod temperature is affected not only by the current, but also by ambient temperature, coordinate position and other factors. A new approach to establishing cathode rod temperature-current model based on nickel electrolysis cell is proposed in this paper. Through extensive analysis, this paper investigates the relationships between rod temperature and current volume, current branch ratio, coordinate position. Based on SPSS regression analysis, a cathode rod temperature-current model of nickel electrolysis cell is established, which is determined by multi-factors. The model is used to estimate the current value on the basis of the temperature on the cathode rod, ambient temperature and coordinate position, which almost agrees with real current value. The models proposed in this paper are of guiding significance to fully acquire the cathode current distribution information of nickel electrolysis cells, improve the current efficiency and reduce energy consumption. *Copyright © 2014 IFSA Publishing, S. L.*

Keywords: Nickel electrolysis cells, Cathode rod current, Temperature distribution on cathode rod, Regression analysis, Modeling method.

1. Introduction

In the process of nickel electrolysis production, the temperature distribution on cathode rod is influenced by ambient temperature, the cathode rod thermal radiation as well as the actual current via the cathode rod. Too high or too low current on cathode rod will be shown in the form of temperature distribution. Therefore, current value can be relatively correctly calculated by accurately monitoring the temperature distribution on cathode rod.

There exists a gradient for cathode rod temperature distribution in nickel electrolysis, so the directly measured temperature on a particular point can not be regarded as the temperature value of a certain cathode rod. Scholars in China introduced heat transfer coefficient and established a wire temperature model [1-3] by heat balance principle while scholars in other countries used CAT-1 system and derived a similar model by data fitting [4]. However, these methods ignored some essential factors affecting wire temperature. Chinese scholars, by means of variable transformation [5-9], changed the wire temperature model from a nonlinear problem into a linear one with the method of linear regression, thereby establishing a new model determined by a number of factors. The application object of the

proposed model in this paper is the cathode rod in a nickel electrolysis plant, which, compared with ordinary wire, bulks up its volume and assumes a hollow cylinder shape.

In this paper, firstly in accordance with the specifications of 20 kA series of nickel electrolysis in a company, the temperature data of the cathode rod is generated at different ambient temperature, current branch ratio (CBR), positions and current with the help of multiple physical fields simulation software COMSOL. SPSS statistics software is used to study the correlation between variables, make regression analysis of processed data [10-13], and deduce a cathode rod temperature-current model based on nickel electrolysis cells, which is used to estimate the current value of nickel electrolysis cathode, thereby getting the current distribution status of the whole electrolysis cell. The access to current distribution data can offer some technical support to the improvement in the efficiency of nickel electrolysis current, the increase in productivity and energy conservation. In addition, fault detection and early warning in the process of nickel electrolysis can be made in order to take timely remedial measures, preventing adverse consequences brought about by too high local temperature on the cathode rod in the process of nickel electrolysis.

2. Regression Analyses of Statistical Methods

The statistics regression software SPSS is applied in this paper to describe quantitatively the mathematical relationship among the variables by offering math equations among variables [14].

2.1. Model Regression

The multivariable linear regression model is a mathematical model dealing with the linear relationship between one dependent variable and more than one independent variable in regression analysis. Math expression is shown as equation (1).

$$y=\beta_0+\beta_1x_1+\beta_2x_2+\ldots+\beta_{n-1}x_{n-1}+\varepsilon, \quad (1)$$

where y is the dependent variable, x_1, $x_2 \ldots x_{n-1}$ are the independent variables, β_0, β_1, $\beta_2 \ldots \beta_{n-1}$ are unknown parameters, and ε is the zero mean random variable. When there are N-pieces of data, equation (1) can be rewritten as equation (2).

$$y_i=\beta_0+\beta_1x_{i1}+\beta_2x_{i2}+\ldots+\beta_{n-1}x_{i,n-1}+\varepsilon_i, \quad (2)$$

where $i=1,2\ldots,N$; $\varepsilon_1,\varepsilon_2\ldots\varepsilon_N$ are the independently distributed in $N(0,\sigma^2)$; and σ is the standard deviation. $\hat{\beta}_0$, $\hat{\beta}_1$, $\hat{\beta}_2 \ldots \hat{\beta}_{n-1}$, the estimate values of β_0, β_1, $\beta_2 \ldots \beta_{n-1}$ are derived using least square method [15]. Finally, equation (3) is referred to as an n-variables linear regression model.

$$\hat{y}=\hat{\beta}_0+\hat{\beta}_1x_1+\hat{\beta}_2x_2+\ldots+\hat{\beta}_{n-1}x_{n-1}, \quad (3)$$

2.2. Statistical Tests of Regression Equation

For the derived regression equation, a test of goodness of fit (TOGOF) and a test of significance are usually conducted, as well as a significance test of regression coefficient, thereby judging the regression effect of the model. If different regression methods are adopted to get the equation to be determined, assumed to be a linear equation or nonlinear one, then the regression effect is quite different. In this case, the optimum regression equation will be chosen by comparing its determination coefficients or adjusted determination coefficients and concomitant probability Sig. value of F-test in different regression ways. Therefore, it is necessary to conduct statistical tests of regression equation to judge whether the fitting model is suitable or not.

2.1.1. Model Evaluation- TOGOF of Regression Equations

TOGOF of the equation is a test of the intensity of sample data points around the regression line, thereby evaluating the representing level of regression equations for sample data. If x is set as independent variable, y as dependent variable, there are mainly two reasons for the difference in the observed values of y: 1) independent variable x is valued differently; 2) effects of other random factors. In TOGOF of the equation, total sum of squares *SST*, regression sum of squares *SSR*, explained sum of squares *SSE* are mainly tested, respectively defined as equation (4), (5) and (6).

$$SST=\sum_{t=1}^{N}(y_t-\overline{y}_t)^2, \quad (4)$$

$$SSR=\sum_{t=1}^{N}(\hat{y}_t-\overline{y}_t)^2, \quad (5)$$

$$SSE=\sum_{t=1}^{N}(y_t-\hat{y}_t)^2, \quad (6)$$

where y_t is the given data; $\hat{y}_t$ is the predicted data; $\overline{y}_t$ is the mean value of the given data y_t. The relationship among these three equations is shown in equation (7).

$$SST=SSR+SSE, \quad (7)$$

SSR refers to variation which can be explained by the equation, *SSE* is the variation which cannot be explained by the equation. It can be seen from the above equation that in a regression equation, the bigger *SSR* is, the smaller *SSE* and the better the goodness of fit of the equation is. The goodness of fit of the regression equation is tested by the coefficient of determination R^2 or adjusted coefficient of determination $\overline{R}^2$ in multiple regressions [11, 16]. As is shown in equation (8) and (9), N is the sample size and k is the number of parameters. R^2 and $\overline{R}^2$ are ranged from 0 to 1. The closer to 1 the value is, the closer relationship between independent variable and dependent variable.

$$R^2 = \frac{SSR}{SST}, \tag{8}$$

$$\overline{R}^2 = 1 - \frac{N-1}{N-k}(1-R^2), \tag{9}$$

2.1.2. Model Validation

Model validation mainly consists of significance test of regression equation (F test) and significance test of regression coefficient (t test).

1) Significance test of regression equation-F test

F test is used to test whether the linear relationship between dependent variable and all independent variables is significant, as well as whether the description of their relationship is appropriate using linear model. The variance analysis method is adopted to research on whether *SSR*, relative to *SSE*, accounts for a larger proportion in *SST*. The null hypothesis of F-test is H_0: $\beta_1 = \beta_2 = \ldots = \beta_{n-1} = 0$, Test statistics is shown in equation (10).

$$F = \frac{SSR/k\text{-}1}{SSE/(N\text{-}k\text{-}1)}, \tag{10}$$

where under the null hypothesis, F~F (n-1,N-n). If H_0 is not true, then F has a tendency to be larger.

2) Significance test of regression coefficients-t test.

T test aims to research on whether there exists a significant linear relationship between dependent variable and every independent variable in the regression equation, namely to examine whether each independent variable can effectively explain the changes of dependent variable and whether they remain in the linear regression equation. T test statistics is shown in equation (11), which obeys the *t*-distribution with the degree of freedom N-n under the condition of null hypothesis H0.

$$t = \frac{\hat{\beta}_i}{S(\hat{\beta}_i)} \quad i = 1, 2, \ldots n-1, \tag{11}$$

When $|t|$ is less than the critical value $t_{\alpha/2}(N-n)$, it indicates that the coefficient does not pass testing. When it is larger than the critical value, it means that the coefficient passes testing.

3. Sample Data Acquisition

The simulation subject is cathode rod of nickel electrolysis cells in 20 kA series at a nickel plant: a hollow copper rod in the shape of cylinder, 1260 mm in length, 18 mm in diameter, 2 mm in wall thickness. Taking into account the actual conditions, each cell is equipped with 40 cathode rods, each having an average current of 0.5 kA. Such factors as wind speed and sunshine have little impact on the cell since it is assembled indoors. In order to simplify the model, the simulation only considers natural convection and heat transfer between the cathode rod and the air around under ideal conditions, ignoring the effect of wind speed and light.

The cathode rod in this paper, consistent with its actual structure, is divided into three sections on average to simulate the actual shunt circuit, with the two connectors on the middle part of the cathode rod respectively representing two nickel ears attached. The physical model is shown in Fig. 1.

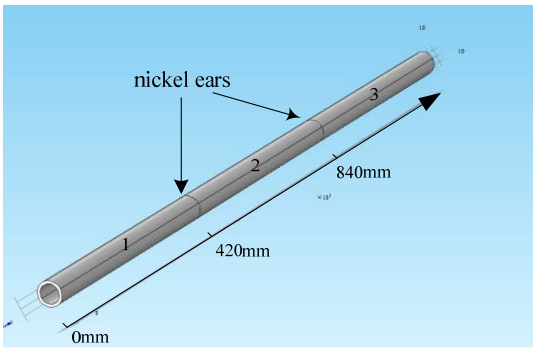

Fig. 1. Schematic of simulation model.

The established cathode rod model is used to make respective simulation under the conditions of different ambient temperature T_0 valued at 40 °C, 45 °C, 50 °C, 55 °C, 60 °C, and different CBR valued at 0.1, 0.3, 0.5, 0.65, 0.7, 0.75, 0.80, 0.85, 0.9, 0.95, generating 10500 groups of sample data. The following is an exploration of modeling methods, taking temperature distribution data corresponding to different CBR as an example, at ambient temperature 40 °C and the current of 0.5 kA which is close to the actual operation conditions. The generated data is as followed in Table 1.

Table 1. Temperature data of Cathode rod at 40 °C, 0.5 KA.

Position	CBR					
(z)	0.1	0.3	0.5	0.7	0.8	0.9
0	47.110	47.240	47.500	47.890	48.134	48.410
0.042	47.088	47.219	47.482	47.876	48.122	48.401
0.084	47.019	47.154	47.426	47.833	48.088	48.376
0.126	46.903	47.046	47.332	47.762	48.030	48.334
0.168	46.737	46.890	47.197	47.658	47.946	48.273
0.210	46.517	46.685	47.020	47.522	47.836	48.192
0.252	46.240	46.425	46.795	47.350	47.697	48.090
0.294	45.896	46.102	46.516	47.136	47.524	47.963
0.336	45.483	45.716	46.182	46.880	47.317	47.812
0.378	44.985	45.249	45.778	46.571	47.067	47.629
0.420	44.397	44.698	45.302	46.206	46.772	47.413
0.462	43.804	44.141	44.816	45.828	46.460	47.177
0.504	43.290	43.655	44.384	45.477	46.161	46.935
0.546	42.852	43.235	44.001	45.151	45.870	46.685
0.588	42.470	42.864	43.654	44.837	45.577	46.415
0.630	42.143	42.541	43.338	44.532	45.279	46.125
0.672	42.256	43.045	44.228	44.968	45.806	41.861
0.714	41.617	42.000	42.767	43.917	44.635	45.450
0.756	41.409	41.773	42.502	43.595	44.279	45.053
0.798	41.228	41.565	42.240	43.251	43.884	44.600
0.840	41.073	41.374	41.977	42.882	43.447	44.088

4. Cathode Rod Temperature-current Relationship Modeling

The environment at nickel electrolysis plant is bad and the electrolytic process is complex. Fig. 2 shows the photos of the part of cell. For the convenience of statement, the current relationship between adjacent pole rods is simplified as shown in Fig. 3. There are two nickel ears on each nickel cathode rod, current flows through the first section $(0 \le z \le 420)$ of anode and cathode rod and the second section $(420 < z \le 840)$, no current on the third section. Assuming the total current through the anode rod is I, which flows to cathode rod through the electrolyte and nickel ears. As is shown in Fig. 3, the relationship of three current is shown in equation (12).

$$I = I_1 + I_2, \tag{12}$$

Fig. 2. Nickel electrolysis cells electrode distribution.

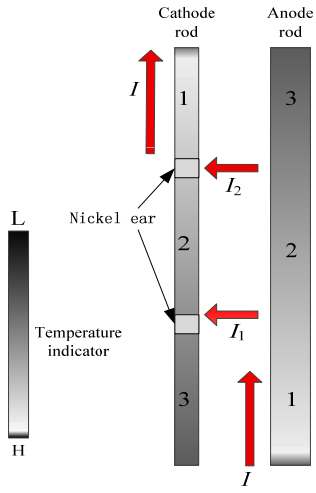

Fig. 3. Schematic of current distribution between poles.

4.1. The Factors Affecting the Temperature on Cathode Rods

In the process of nickel electrolysis, the temperature T on each point of cathode rod is influenced by ambient temperature T_0 and the percentage of the current flowing initially from anode rod to cathode rod (CBR, denoted as i_r), as well as the total current I of the cathode rod. As the coordinate position changes, cathode temperature will vary, namely the coordinate position will also affect the cathode temperature. i_r is defined in equation (13).

$$i_r = \frac{I_1}{I}, \tag{13}$$

In practice, because the cathode temperature is influenced by ambient temperature to a great extent, it can be considered that it is ΔT, the difference value that other variables affect. Let ΔT be equal to the difference value between T and T_0, i.e. $\Delta T=T-T_0$. ΔT is regarded as the dependent variable of regression model. Through the data analysis, the function relationship corresponding to the dependent variable and each independent variable is found so that the relationship between each processed independent variable and dependent variable is approximately linear, thereby adopting the linear regression method to model.

4.1.1. The Influence of the Total Current *I* on the Temperature Difference ΔT

By Joule's law, the heat generated in the current-carrying conductor, the Joule heat Q is proportional to the square of i, the resistance of a conductor R, time t, as is shown in equation (14).

$$Q = i^2 * R * t, \tag{14}$$

In respect of the same cathode rod, under the same conditions, the greater the current value is, the more the Joule heat is generated.

Fig. 4 is the scatter diagram indicating that ΔT changes with the square of the current I^2 at the same position $z = 420\,mm$, with i_r respectively valued at 0.1, 0.3, 0.5, 0.7, 0.8, 0.9. Apparently, there is a significant linear relationship between ΔT and I^2.

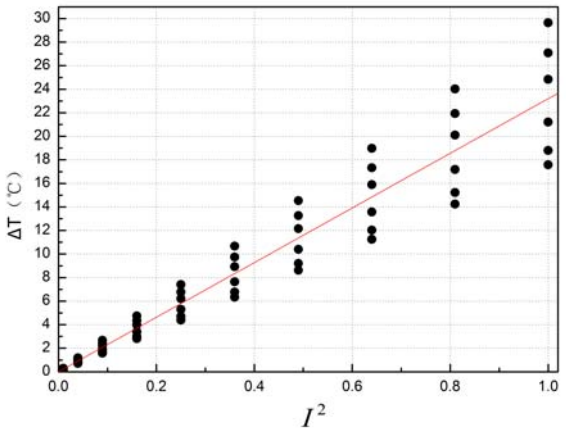

Fig. 4. Relationship between ΔT and I^2.

4.1.2. The Effect of CBR on Temperature Difference ΔT

As is seen from Fig. 3, when the total current I on anode rod reaches the first nickel ear through electrolyte, the current I_1 flows into the first section of the cathode rod. Similarly, the residual current I_2 on anode rod flows into the cathode rod through electrolyte and the second nickel ear, so the current through the first section of the cathode rod corresponds to the total current I. The current through the cathode rod flows from bottom to top, gradually increasing. The heat produced in the first section of the cathode rod will transfer to the second section, until the two sections reach thermal equilibrium. The heat transmitted from the first section of the cathode rod to the second section depends on I_1. The greater I_1 is, the larger i_r is. The less temperature difference between the first section of the cathode rod and the second section, the less heat is transmitted. Fig. 5 is the change trend indicating that ΔT changes with IR at the same position $z = 420\,mm$, with the total current I respectively valued at 0.1 kA, 0.3 kA, 0.5 kA, 0.7 kA, 0.9 kA. ΔT does not decrease with the increase in i_r, because the greater i_r is, the more current I_1 flows into the cathode from the anode. The heat produced by its total current through the cathode rod is far greater than the transferred heat. Similar to the previous section, there is a clear linear relationship between ΔT and i_r^2.

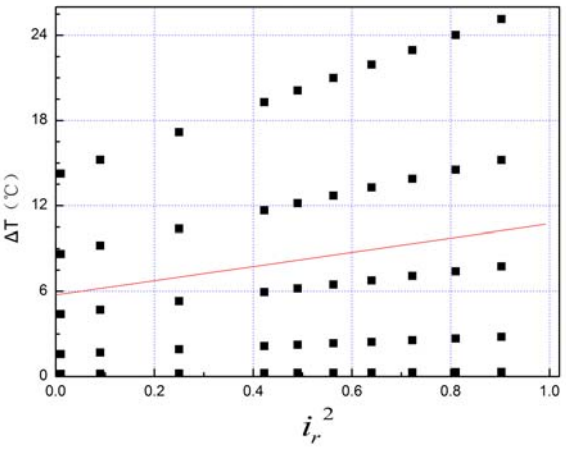

Fig. 5. Relationship between ΔT and i_r^2.

4.1.3. Effect of Position z on Temperature Difference ΔT

ΔT on each point of the cathode rod changes with position z. With the total current flowing through cathode rod $I = 0.5kA$, i_r is respectively valued at 0.1, 0.3, 0.5, 0.7, 0.8, 0.9, the relationship between ΔT and z is shown in Fig. 6.

It can be seen from the overall trend in Fig. 6 that there is not obvious linear relationship between ΔT and position z or z^2. The temperature on the cathode rod gradually decreases with the increase in z value, but the temperature distribution on the first and the second section presents curves of different shapes corresponding to IR changes. In Fig.6 (a), the three scatter diagrams above correspond to three kinds of

temperature distribution in the case of i_r greater than or equal to 0.7, the other three scatter diagrams below correspond to three kinds of temperature distribution in the case of i_r less than 0.7. Obviously, the concavity-convexity property of the curve in the second section of the cathode rod is very obvious, which can serve as a basis on which to choose the model below.

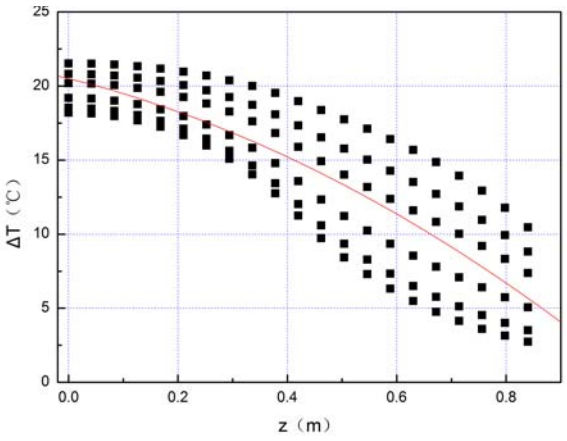

(a) ΔT - z relationship curve

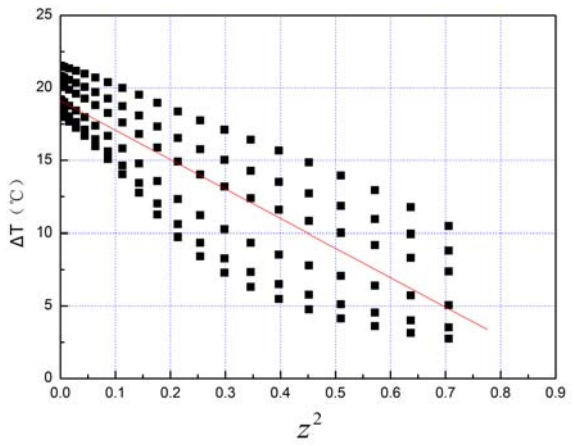

(b) ΔT - z^2 relationship curve

Fig. 6. Relationship between ΔT and z .

To improve the accuracy of the model, the segmented modeling method is essential: if $0 \le z \le 0.42$, convex function is between ΔT and z; if $0.42 < z \le 0.84$, two different situations need to be dealt with separately. If i_r=0.1, 0.3, 0.5, concave function is between T and z; if i_r=0.7, 0.8, 0.9, convex function is between ΔT and z. Through calculation, it is known that if i_r=0.681, the relationship between ΔT and z is completely linear, which can be used as the transition point from concavity to convexity. As a result, the second section of the cathode rod is segmented on the basis of i_r value. Fig. 7-Fig. 9 respectively represent the relationship curves between the temperature difference ΔT and power function of z in the case of $z \in [0,0.42]$ and $i_r \in (0.1,1)$, $z \in (0.42,0.84]$ and $i_r \in (0,0.681)$, $z \in (0.42,0.84]$ and $i_r \in (0.681,1)$ (respectively recorded as intervals 1, 2, 3).

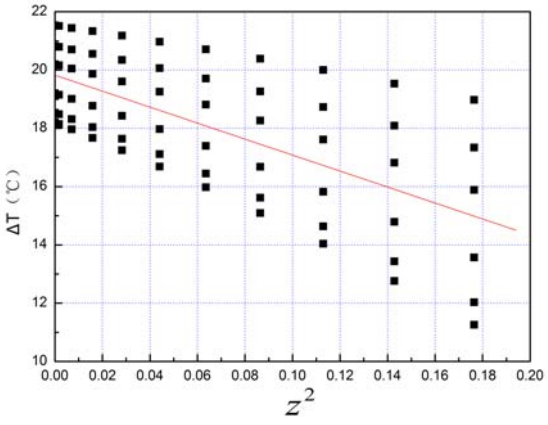

Fig. 7. Relationship between ΔT and z^2 in Interval 1.

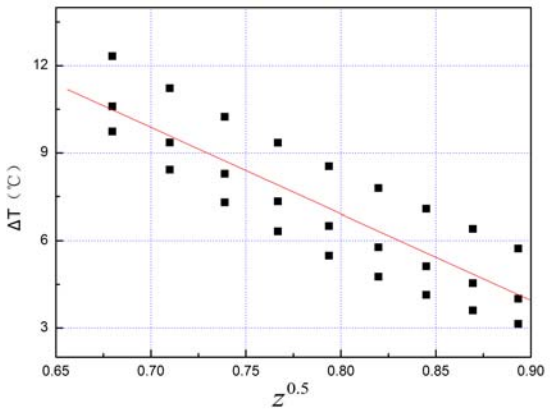

Fig. 8. Relationship between ΔT and $z^{0.5}$ in Interval 2.

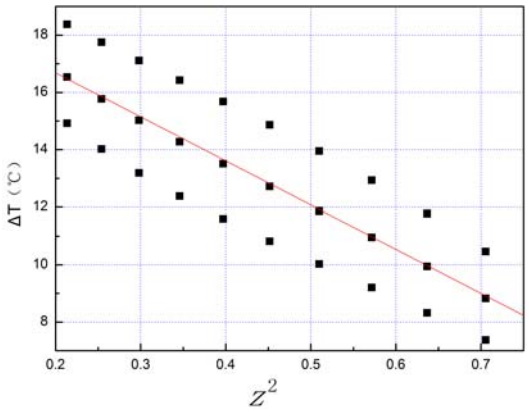

Fig. 9. Relationship between ΔT and z^2 in Interval 3.

4.1.4. Model Regression

Fig. 4 ~ Fig. 9 show that ΔT is not in linear relationship with I, z and i_r, but has an approximate linear relation to I^2, ${i_r}^2$, z^2 and $z^{0.5}$. First derive regression models respectively with a multivariable linear regression method, which are shown in equation (15), (16), (17):

If $z \in [0,420]$, $i_r \in (0,1)$, let $z = z_1$, then

$$\Delta T_1 = 29.340 I^2 + 3.591 {i_r}^2 - 16.552 {z_1}^2 + 0.001 z_1 - 0.934, \quad (15)$$

If $z \in (420,840]$, $i_r \in (0,0.681)$, let $z = z_2$, $i_r = i_{r1}$, then

$$\Delta T_2 = 12.048 {I_2}^2 + 7.043 {i_{r1}}^2 - 18.035 {z_2}^{0.5} + 13.128, \quad (16)$$

If $z \in (420,840], i_r \in (0.681,1)$, let $z = z_2, i_r = i_{r2}$, then

$$\Delta T_3 = 19.560 {I_2}^2 + 7.043 {i_{r2}}^2 - 5.877 {z_2}^2 - 4.316 z_2 + 1.134, \quad (17)$$

Coefficients of determination of model in interval 1~3 are respectively $R_1 = 0.993$, $R_2 = 0.945$, $R_3 = 0.980$. Adjusted coefficients of determination are $\overline{R}_1 = 0.985$, $\overline{R}_2 = 0.892$, $\overline{R}_3 = 0.961$ respectively. The coefficients of determination and adjusted coefficients are greater than 0.8 and close to 1, which indicates good model fitting. At the same time, concomitant probability of F test is 0, the coefficients and constant corresponding to I^2, i_r, z^2, $z^{0.5}$ and z in the model and concomitant probability of t test are close to 0, both passing the test of significance. The above analysis shows regression equation and regression coefficient are statistically significant. It is suitable to use this model to describe the relationship among ΔT, I, i_r, z.

4.1.5. Model Simplification

As can be seen from the upper chapter, the model is segmented according to coordinate position z and i_r. If $z \in [0,420]$ mm, because i_r in equation (15) does not affect the concavity-convexity property of the curve, i_r in equations (16) and (17) is included. Insert i_{r1} and i_{r2} in equations (16) and (17) to equation (15) in sequence, and the new equations (18), (19) will be obtained respectively, retaining only the unknown variable I, which are simpler and more suitable for practical application. The present current I can be derived from the new model, directly based on any two points z_1 and z_2 on the cathode rod and the temperature difference ΔT_1 and ΔT_2. If the temperature distribution on the second section of the cathode rod is a concave curve, equation (18) is selected; on the contrary, if the temperature distribution on the second section of the cathode rod is a convex curve, equation (19) is adopted.

$$\begin{aligned} &98.437 I^4 - (3.355 \Delta T_1 + 55.533 z_1^2 \\ &-0.003 z_1 - 54.411) I^2 + \Delta T_2 - \\ &1.961 \Delta T_1 - 32.463 z_1^2 + 0.002 z_1 \\ &+18.035 z_2^{0.5} - 14.960 = 0 \end{aligned}, \quad (18)$$

$$\begin{aligned} &159.814 I^4 - (5.447 \Delta T_1 + 90.158 z_1^2 \\ &-0.005 z_1 - 52.457) I^2 + \Delta T_3 - \\ &1.961 \Delta T_1 - 32.463 z_1^2 + 0.002 z_1 \\ &+5.877 z_2^2 + 4.316 z_2 - 2.966 = 0 \end{aligned}, \quad (19)$$

5 Experimental Results and Analysis

In order to verify the above derivation model, an infrared camera is used for a nickel electrolysis cell to be captured. The infrared image resolution is 640×480. The camera is set with a fixed gain for a definite relationship between the gray scale value and temperature.

Infrared images collected on the scene are shown in Fig. 10. The ambient temperature T_0 is measured at 40.2°C and the length of the cathode rod is 1260 mm, with the anode and cathode arranged alternately from left to right. The close-range shooting photo is selected to achieve a higher temperature resolution. When the image is captured, the current of corresponding cathode rods is measured by a clamp current meter with precision of 0.5 %. The mean values of the total current I through cathode rod 1~4 are respectively 520 A, 610 A, 540 A, 480 A, and i_r are 0.33, 0.52, 0.48, 0.73.

5.1. Retrieve of Temperature Information on the Cathode Rod

An image processing method is used to retrieve the gray scale value of the temperature distribution on each point of the cathode rod. As is shown in Fig. 10, the infrared images with annotation of dots and dashes are cathode rods, numbered 1~4 from the left to the right.

When retrieving data, start from z=0, the top position of each cathode rod. The corresponding relationship between the pixel and the specific position can be obtained by the distribution of image pixel and actual length of the cathode rod: 315 pixel corresponds to 1260 mm.

As is mentioned above, the current flows through the first and the second section of the cathode rod only, so the data is derived from two-thirds of the cathode only, namely 0~840 mm.

The relationship between gray level of the image and the temperature is basically linear [17], linear equation can be used to fit out the relation between them. Combined with the parameters setting of the camera, after temperature calibration, the relationship between thermal infrared image grayscale value G and temperature *T* calibration can be expressed as:

$$T = aG + b, \tag{20}$$

where $a = 0.226$, $b = 38.709$. Thereby, the temperature value on each point of the cathode can be retrieved.

A model validation experiment is made according to the temperature distribution data on the four cathode rods denoted in Fig. 10. The cathode current derived from equations (18) and (19) is shown in Table 2.

Table 2. Comparative analysis of current through cathode rod.

z	gray level				T(°C)				calculated value (A)			
	1	2	3	4	1	2	3	4	1	2	3	4
0	48	56	38	28	49.5	51.3	47.3	45.0	530	592	538	494
14	48	59	36	31	49.5	52.0	46.8	45.6	510	584	493	401
28	45	56	39	29	48.8	51.4	47.6	45.3	519	613	510	398
42	47	58	38	31	49.4	51.8	47.3	45.7	517	583	553	438
56	45	56	41	31	48.8	51.4	47.9	45.8	521	586	465	430
70	42	58	43	37	48.2	51.8	48.4	47.0	526	611	584	448
84	41	60	42	36	48.0	52.2	48.2	46.9	528	584	557	464
98	39	58	43	34	47.6	51.9	48.5	46.4	518	577	522	404
112	40	58	41	35	47.8	51.9	47.9	46.7	514	608	488	426
126	39	61	44	32	47.6	52.6	48.6	46.0	491	587	510	479
140	43	61	39	35	48.4	52.5	47.6	46.7	486	639	558	444
154	42	61	45	36	48.3	52.5	48.9	46.8	470	630	578	426
168	41	60	40	32	47.9	52.2	47.7	46.0	501	620	554	405
182	41	58	45	36	48.0	51.7	48.8	46.9	511	559	527	417
196	41	58	39	34	48.1	51.8	47.5	46.5	472	536	438	425
210	41	57	42	34	47.9	51.5	48.2	46.3	512	630	613	475
224	38	56	39	34	47.2	51.3	47.6	46.5	521	573	515	481
238	39	55	40	33	47.6	51.2	47.7	46.1	529	559	479	445
252	38	57	40	34	47.3	51.6	47.6	46.5	466	603	533	486
266	38	56	41	31	47.2	51.4	48.0	45.7	526	611	509	490
280	38	55	38	31	47.3	51.2	47.3	45.6	494	593	563	486
294	37	56	38	31	47.0	51.5	47.4	45.6	458	572	560	475
308	37	54	40	33	47.0	51.0	47.8	46.2	490	574	519	482
322	37	53	40	30	47.1	50.8	47.7	45.4	501	637	584	510
336	35	52	35	30	46.7	50.6	46.5	45.4	454	590	532	480
350	34	52	36	29	46.4	50.4	46.7	45.2	508	558	461	453
364	35	52	37	29	46.7	50.5	47.1	45.3	467	550	448	431
378	33	50	37	31	46.2	50.0	47.1	45.7	506	597	568	477
392	37	47	33	24	47.0	49.2	46.1	44.1	534	579	537	451
406	35	48	31	24	46.6	49.5	45.7	44.2	536	538	485	476
420	36	46	31	23	46.9	49.1	45.6	43.9	504	596	578	429
434	34	47	31	22	46.3	49.3	45.7	43.6	380	510	475	376
448	34	47	25	21	46.4	49.4	44.4	43.4	268	398	366	338
462	28	49	29	26	45.0	49.7	45.2	44.5	227	414	385	360
476	28	47	28	25	45.1	49.4	45.0	44.3	241	343	317	350
490	25	46	27	25	44.3	49.0	44.9	44.3	241	363	323	358
504	24	46	26	24	44.2	49.0	44.5	44.2	248	401	324	361
518	24	45	26	23	44.1	48.9	44.7	43.8	183	382	351	379
532	25	43	26	27	44.4	48.4	44.5	44.7	203	370	286	341
546	22	45	24	22	43.8	48.8	44.0	43.7	259	435	374	364
560	24	44	24	22	44.1	48.7	44.2	43.7	248	388	381	415
574	24	43	23	21	44.2	48.4	44.0	43.4	176	370	348	377
588	22	42	24	26	43.7	48.3	44.2	44.6	202	390	384	349
602	22	40	24	23	43.7	47.7	44.0	44.0	193	428	417	375
616	22	40	21	20	43.6	47.9	43.5	43.3	171	382	373	348
630	20	39	21	23	43.3	47.6	43.5	44.0	179	380	328	386
644	20	41	20	17	43.2	47.9	43.2	42.6	241	371	310	377
658	21	38	20	20	43.4	47.2	43.3	43.3	217	364	305	390
672	21	38	20	17	43.4	47.3	43.2	42.6	176	346	300	398
686	19	39	22	17	43.0	47.5	43.6	42.6	193	445	370	416
700	17	36	20	19	42.6	46.8	43.1	42.9	228	411	349	399
714	20	36	21	17	43.2	46.9	43.5	42.7	184	437	428	417
728	17	37	19	18	42.6	47.2	43.0	42.8	135	429	372	385
742	18	37	19	15	42.7	47.1	43.0	42.1	203	376	330	412
756	17	35	20	17	42.5	46.7	43.1	42.5	159	411	352	409
770	17	37	18	13	42.7	47.0	42.7	41.6	137	386	362	423
784	15	34	17	17	42.1	46.4	42.5	42.6	163	410	328	429
798	17	33	20	13	42.5	46.3	43.1	41.6	123	418	338	414
812	19	31	16	11	42.9	45.8	42.3	41.1	184	459	402	425
826	19	31	13	7	43.0	45.8	41.7	40.3	201	401	349	390
840	20	30	13	7	43.2	45.6	41.7	40.3	204	429	367	425

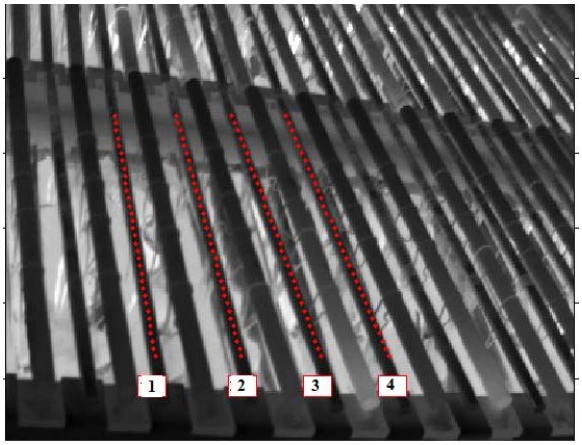

Fig. 10. Marked infrared image.

As can be seen from Table 2, compared with the simulation data, the measured temperature data has larger fluctuations. The main reasons are as followed. First, the contact section of cathode rod and bus is affected by electric heating of contact resistance, leading to the exceptional temperature data in the section. Second, the contact section of nickel ear and cathode rod is influenced by the oxidation degree of the contact area, resulting in large temperature data deviation. Third, different degrees of surface oxidation lead to deviation of radiation rate on different sections of the same cathode rod, as a result of which the temperature measurement data fluctuates.

Taking into account the three factors mentioned above, the data on the contact points of cathode rod and bus as well as nickel ear is excluded. The data fluctuation, caused by radiation rate deviation, can be improved through follow-up study, using visible light and infrared images fusion method for real-time radiation rate correction. The corresponding temperature distribution on four cathode rods, after the fluctuation data is eliminated, is shown in Fig. 11. The dotted lines in the figure represent measured data and the smooth curves are trend lines. These trend lines aim to decide which model to use according to the concavity-convexity property of temperature distribution curve on the second section. In essence, the process of obtaining trend lines is the process of function regression. Equation (2) presented previously can be simplified as the following matrix form:

$$\begin{cases} Y = X\beta + \varepsilon \\ \varepsilon \sim N(0, \sigma^2 I_n) \end{cases}, \tag{21}$$

where I_n is the n-order identity matrix. Using least squares method:

$$\hat{\beta} = (X^T X)^{-1} X^T Y, \tag{22}$$

Introduce the independent variable into the regression equations and derive estimated values for the dependent variable:

$$\hat{Y} \triangleq (\hat{y}_1, \hat{y}_2, \ldots \hat{y}_n) = X\hat{\beta}, \tag{23}$$

namely, the value on every point of the trend line.

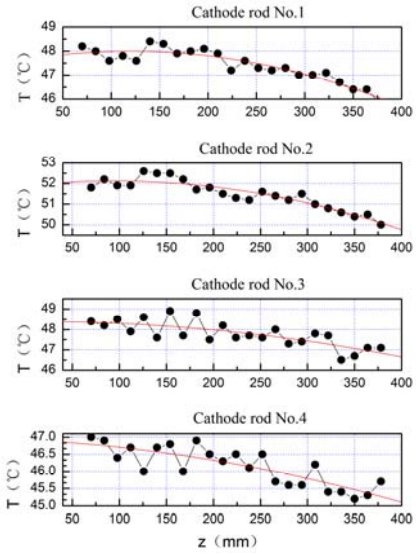

(a) Temperature distribution on the first section of cathode rod

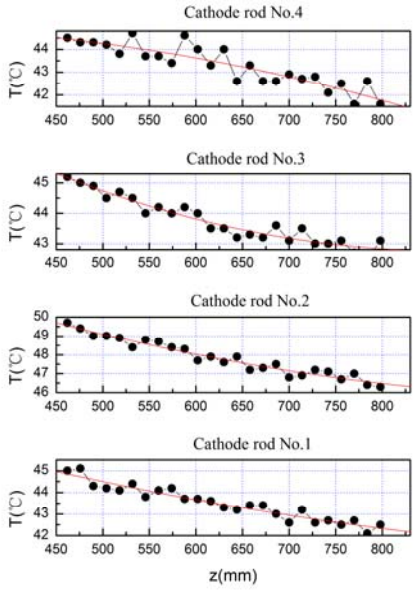

(b) Temperature distribution on the second section of cathode rod

Fig. 11. Temperature distribution on Cathode rod.

5.2. Estimate of Total Current and CBR

It can be seen from the trend of temperature distribution data in Fig. 11 that the second section of cathode rod No.1~3 is of a concave curve shape, so

equation (18) should be used to get the estimated current value I. While the second section of cathode rod is of a convex curve shape, so equation (19) should be used to get the value. Then the results are introduced into equation (15) for estimated value i_r.

As is mentioned above, fluctuations of the measured temperature data caused by radiation rate deviation will lead to less accuracy in model identification. If the disturbance is a zero mean random signal, a multipoint arithmetic mean method is presented in this paper to get the total current I' and CBR i_r' of each cathode rod. The results of error analysis are shown in Table 3 and Table 4.

Table 3. Error analysis of total current.

Cathode rod current				
	1	**2**	**3**	**4**
I'	504	589	528	452
I	520	610	540	480
Error	-3.11	-3.38	-2.27	-5.74

Table 4. Error analysis of CBR.

Cathode rod current				
	1	**2**	**3**	**4**
i_r'	0.39	0.67	0.67	0.85
i_r	0.33	0.52	0.48	0.73
Error	19.13	28.36	39.03	16.95

Seen from the results of error analysis, it is obvious that by the model established in this paper the error in the calculation of the total current is less than 6 %, while the CBR error is relatively large, with the maximum error close to 40 %. Therefore, cathode current calculation results are close to the actual value, with less errors, and can reflect the current distribution on each cathode rod of electrolysis cell more accurately, which is of practical value.

6. Conclusion

1) In this paper physical field simulation software is used to generate the sample data and study the relationship between the temperature difference of cathode rod and total current, CBR and position. An analytic expression model is established by the linearization of function. The statistical index in the model reaches the standard and has statistical significance.

2) Two simplified models are established with the CBR for the demarcation point. Models are selected and the total current through cathode rod is estimated according to the concavity-convexity property of the temperature distribution curve on the second section of cathode rod. The calculated results of the models are relatively close to the actual current value. The models proposed in this paper are of guiding significance to fully acquire the cathode current distribution information of nickel electrolysis cells, improve the current efficiency and reduce energy consumption.

3) The impact of fluctuations of the temperature data caused by radiation rate deviation is expected to be reduced by image fusion methods, so as to further improve the precision of model identification

References

[1]. Lu Xinmiao, Zeng Yi, Sheng Gehao, et al, Line dynamic capacity error analysis based on conductor temperature models, *East China Electric Power*, Vol. 35, Issue 12, 2007, pp. 47-49.

[2]. Lu Xinmiao, Ren Lijia, Sheng Gehao, et al, Dynamic line rating systems based on conductor tension, *East China Electric Power*, Vol. 36, Issue 12, 2008, pp. 30-33.

[3]. IEEE Standard 738-2006 IEEE standard for calculating the current-temperature relationship of bare overhead conductors, *IEEE Standards Association*, 2006.

[4]. J. K. Raniga, R. K. Rayudu, Dynamic rating of transmission lines: a New Zealand experience, in *Proceedings of Power Engineering Society Winter Meeting*, pp. 2403-2409, 2000.

[5]. Cai Congzhong, Wen Yufeng, Zhu Xingjian, et al, Quantitative prediction of mechanical properties of 7005 Al alloys from processing parameters via support vector regression, *The Chinese Journal of Nonferrous Metals*, Vol. 20 Issue 2, 2010, pp. 323-328.

[6]. Wang Huiwen, Meng Jie, Predictive modeling on multivariate linear regression, *Journal of Beijing University of Aeronautics and Astronautics*, Vol. 33, Issue 4, 2007, pp. 500-504.

[7]. Wang Huiwen, Li Nan, Linear regression analysis for normal distribution-valued data based on complete information, *Journal of Beijing University of Aeronautics and Astronautics*, Vol. 28, Issue 10, 2012, pp. 1275-1279.

[8]. Tu Jun, Li Yan-Ming, Liu Cheng-Liang, A vehicle traveling time prediction method based on grey theory and linear regression analysis, *Shanghai Jiaotong University,* Vol. 14, Issue 4, 2009, pp. 486-489.

[9]. Ren Lijia, Sheng Gehao, Zeng Yi, et al, A conductor temperature model based on dynamic line rating technology, *Automation of Electric Power Systems*, Vol. 33 Issue 5, 2009, pp. 40-44.

[10]. Zhang Lingke, Wang Zhongyuan, Guo Wenjuan, Application of SPSS in trajectory consistency test and data analysis, *Journal of Nanjing University of Science and Technology*, Vol. 30, Issue 2, 2006, pp. 209-212.

[11]. L. Billard, E. Diday, Regression analysis for interval-valued data, *Data Analysis, Classification and Related Methods, Springer*, Belgium, 2000, pp. 369-374.

[12]. L. Billard, E. Diday, Symbolic regression analysis, *Classification, Clustering, and Data Analysis*, 2002, pp. 281-288.

[13]. Liu Minghao, Ren Changming, Nan Li, Research and realize on the regression analysis for forecasting the anterior chamber diameter, *Electronic Measurement Technology*, Vol. 30, Issue 11, pp. 35-39.
[14]. Zhang Hui, Shou Guochu, Hu Yihong, Radio signal forecast for mobile network, *Journal of Electronic Measurement and Instrument,* Vol. 22, Issue 4, 2008, pp. 44-48.
[15]. R. Verde, A. Irpino, Ordinary least squares for histogram data based on Wasserstein distance, in *Proceedings of COMPSTAT*, 2010, pp. 581-588.
[16]. Yu Zhongqi, Zhao Yixi, Lin Zhongqin, Evaluation parameter of drawability of automotive aluminum alloy sheets, *The Chinese Journal of Nonferrous Metals*, Vol. 14, Issue 10, 2004, pp. 1689-1693.
[17]. Xu Yonghua, Wu Min, Cao Weihua, et al, Dynamic calibration algorithm for temperature profile of blast furnace based on statistical distribution of image grey scale, *Metallurgical Industry Automation*, Vol. 3, 2007, pp. 40-43.